Suppressors of *mdm20* in Yeast Identify New Alleles of *ACT1* and *TPM1* Predicted to Enhance Actin-Tropomyosin Interactions

Jason M. Singer, Greg J. Hermann[1] and Janet M. Shaw

Department of Biology, University of Utah, Salt Lake City, Utah 84112

Manuscript received March 20, 2000
Accepted for publication June 9, 2000

ABSTRACT

The actin cytoskeleton is required for many aspects of cell division in yeast, including mitochondrial partitioning into growing buds (mitochondrial inheritance). Yeast cells lacking *MDM20* function display defects in both mitochondrial inheritance and actin organization, specifically, a lack of visible actin cables and enhanced sensitivity to Latrunculin A. *mdm20* mutants also exhibit a temperature-sensitive growth phenotype, which we exploited to isolate second-site suppressor mutations. Nine dominant suppressors selected in an *mdm20/mdm20* background rescue temperature-sensitive growth defects and mitochondrial inheritance defects and partially restore actin cables in haploid and diploid *mdm20* strains. The suppressor mutations define new alleles of *ACT1* and *TPM1*, which encode actin and the major form of tropomyosin in yeast, respectively. The *ACT1* mutations cluster in a region of the actin protein predicted to contact tropomyosin, suggesting that they stabilize actin cables by enhancing actin-tropomyosin interactions. The characteristics of the mutant *ACT1* and *TPM1* alleles and their potential effects on protein structure and binding are discussed.

In mitotically dividing yeast cells, the actin cytoskeleton is organized into two different types of filament-based structures, cortical actin patches that cluster in the growing daughter cell (bud) and polarized actin cables that align along the mother-bud axis (Botstein *et al.* 1997). Actin patches and cables perform numerous functions required for the generation of new buds and the subsequent events of cell division (Botstein *et al.* 1997). At the beginning of the cell cycle, actin is required for both bud site selection and bud emergence. The actin cytoskeleton also plays a central role in the establishment of cell polarity, which in turn sets up directed secretion and growth of the bud. Proper mitotic spindle orientation requires actin function. Finally, actin is a component of the actomyosin ring, which plays a critical role in cytokinesis.

Recent studies indicate that actin is also involved in the inheritance of cellular organelles such as vacuoles (Hill *et al.* 1996; Catlett and Weisman 1998; Wang *et al.* 1998) and mitochondria (Drubin *et al.* 1993; Lazzarino *et al.* 1994; Simon *et al.* 1995, 1997; Hermann *et al.* 1997; Boldogh *et al.* 1998; Hermann and Shaw 1998) during yeast budding. Treatment with the actin-disrupting drug, Latrunculin A (Lat-A), and mutations in the *ACT1* gene have been shown to block the inheritance of mitochondria (Simon *et al.* 1995; Boldogh *et al.* 1998) and vacuoles (Hill *et al.* 1996) during division. In addition, a type V myosin, Myo2p, is proposed to be a component of the vacuole inheritance machinery (Hill *et al.* 1996; Catlett and Weisman 1998). Although none of the known yeast myosins appear to be essential for mitochondrial inheritance (Simon *et al.* 1995), mitochondrial membranes are found closely aligned with actin cables *in vivo* (Drubin *et al.* 1993) and purified mitochondria exhibit ATP-dependent binding and transport along stabilized actin filaments *in vitro* (Lazzarino *et al.* 1994; Simon *et al.* 1995).

Studies of the yeast *MDM20* gene provide additional support for the role of actin cables in mitochondrial transport. *MDM20* encodes a low abundance 93-kD cytoplasmic protein required for efficient mitochondrial inheritance at all temperatures (Hermann *et al.* 1997; Hermann 1998). At elevated temperatures (>34°), *MDM20* becomes essential for growth (Hermann 1998). The mitochondrial inheritance defect in *mdm20* mutants appears to result from a primary defect in actin organization since these cells also lack visible actin cables (Hermann *et al.* 1997). The actin cable defect in *mdm20* cells is similar to that observed in *tpm1* mutants lacking the actin filament-binding protein, tropomyosin 1 (Liu and Bretscher 1989). In muscle cells, tropomyosin regulates myosin-actin interactions during muscle contraction. In nonmuscle cells like yeast, tropomyosin is thought to function in the assembly and/or stabilization of actin cables. Although *TPM1* and *MDM20* encode proteins with unrelated structures, extra copies of

Corresponding author: Janet Shaw, Department of Biology, University of Utah, 257 S. 1400 E., Salt Lake City, UT 84112-0840.
E-mail: shaw@bioscience.utah.edu

[1] *Present address:* Fred Hutchinson Cancer Research Center, 1100 Fairview Ave. N., A3-013, Seattle, WA 98109-1024.

TPM1 suppress actin cable and mitochondrial inheritance defects caused by *mdm20*, and *tpm1* and *mdm20* mutations are synthetically lethal (Hermann *et al.* 1997). In addition, *MDM20* and *TPM1* display a similar pattern of genetic interactions; mutations in both genes result in synthetic lethal phenotypes when combined with mutations in *BEM2* (encodes a GTPase activating protein required for bud emergence; Bender and Pringle 1991; Peterson *et al.* 1994) and *MYO2* (encodes a type V myosin; Johnston *et al.* 1991; Cheney *et al.* 1993). These data suggest that Mdm20p and Tpm1p act in the same or parallel pathways to control the assembly or stabilization of actin cables.

Interactions between a large number of different genes (including *TPM1*, *MYO2*, and *BEM2*) have been shown to play a role in yeast actin assembly and function (Liu and Bretscher 1992; Wang and Bretscher 1995; Botstein *et al.* 1997). In an effort to determine how *MDM20* fits into this network of genes, we selected dominant suppressors of the *mdm20* temperature-sensitive growth defect. The suppressor mutations we recovered all fall within the *ACT1* and *TPM1* genes. Our findings raise the possibility that Mdm20p cooperates with the most central elements of actin cables, perhaps modulating the interaction between actin and tropomyosin.

MATERIALS AND METHODS

Yeast strains, media, and genetic techniques: *Saccharomyces cerevisiae* strains used in this study are derived from the FY strain background (Winston *et al.* 1995) and are listed in Table 1. Standard yeast genetic techniques were used (Sherman *et al.* 1986). Rich medium (YPDextrose) and synthetic medium (SDextrose) were prepared as described (Sherman *et al.* 1986). High salt medium used to detect osmotic sensitivity was made by supplementing synthetic medium with 0.9 M NaCl (Chowdhury *et al.* 1992).

Isolation of suppressor mutations: The diploid strains JSY1371 and JSY1372 (Table 1) were used to obtain pseudorevertants and are homozygous for *mdm20*Δ and *mdm20-1*, respectively. The *mdm20*Δ disruption eliminates 740 of 796 codons of the *MDM20* open reading frame (ORF; Hermann *et al.* 1997). *mdm20-1* is also a severe loss-of-function allele but, unlike *mdm20*Δ, permits the expression of a largely intact protein. It contains two single base pair deletions in codons 749 and 750 of the predicted coding region, resulting in a frameshift that introduces a premature stop at codon 750 (Hermann 1998). Both *mdm20*Δ and *mdm20-1* cause temperature-sensitive lethality at 37°.

To obtain dominant pseudorevertants, we selected spontaneous suppressors arising in the two *mdm20/mdm20* strains described above. Following the method of Adams and Botstein (1989), multiple, independently inoculated 2-ml cultures of JSY1371 or JSY1372 were grown overnight at the permissive temperature (25°). Each individual culture was used to seed a single YPD plate with approximately 3×10^6 cells. After 4 days at the nonpermissive temperature (37°), plates were examined for spontaneous pseudorevertants. Temperature-resistant colonies (≤1 from each plate) were isolated and retested for suppression of the 37° growth defect, while at the cellular level, the strains were examined for changes in their actin organization and mitochondrial inheritance phenotypes (see below). The pseudorevertants were also checked for new phenotypes including cold sensitivity, Lat-A sensitivity, and salt/osmotic sensitivity. Suppressor mutations isolated in the homozygous *mdm20-1/mdm20-1* strain were tested for their ability to suppress the *mdm20* disruption allele (*mdm20*Δ).

Genetic and molecular characterization of suppressor mutations: Recombination frequencies were used to evaluate the potential linkage of *mdm20* suppressor mutations to the *ACT1* and *TPM1* loci. To generate a marked strain for the *ACT1* linkage analysis, the *HIS3* selectable marker was integrated between the *ACT1* and *YPT1* loci in JSY1340 (genotypically identical to JSY3094, Table 1), creating JSY3079 (Table 1). Correct integration into the 5′-flanking DNA of the *ACT1* locus was verified by PCR, using a primer pair that hybridized to the *HIS3* and *ACT1* coding sequences. The *TPM1* linkage analysis was performed with strain JSY1081, containing a *HIS3* disruption of the *TPM1* coding region (Hermann *et al.* 1997; the original disruption strain is JSY707, isogenic to JSY1081, Table 1).

The existence of mutations at the *TPM1* or *ACT1* loci in *mdm20* suppressor strains was verified by DNA sequencing. Genomic DNA was isolated from each *mdm20* suppressor mutant, and the ORF plus ≥475 bp of flanking DNA were PCR amplified from each gene. Purified amplification products were sequenced by the University of Utah DNA sequencing facility. Sequence analysis was performed using DNA* software (DNAStar, Madison, WI).

To verify the DNA sequence prediction that the *DMT2-3/TPM1-5* mutation causes seven amino acids to be added the Tpm1p N terminus, mutant Tpm1 protein was purified from strain JSY3315 as previously described (Drees *et al.* 1995) and partially sequenced. Fourteen cycles of Edman degradation were performed by the University of Utah DNA and peptide facility.

Phenotypic characterization of suppressor mutations: Growth phenotypes of mutant and wild-type strains were compared by a serial dilution assay. Overnight cultures grown in YPD were diluted in fresh medium and grown to midlog phase. The cells were washed once and diluted in series to concentrations ranging from $\sim 1.3 \times 10^7$ cells/ml to 165 cells/ml. After spotting 5 μl of each dilution onto YPD medium, identical plates were incubated for 3 days at 25° and 37°.

The actin cytoskeleton in *mdm20* suppressor strains was visualized with 0.5 μM Alexa568 phalloidin (Molecular Probes, Eugene, OR) following the method of Adams and Pringle (1991) with the exception that fixed cells were stained on ice for 1 hr as suggested by Karpova *et al.* (1998). Stained and washed cells were maintained on ice until mounted for microscopy. Actin cables are most easily observed in cells with small to medium buds. Therefore, only cells in this stage were scored for the presence or absence of cable(-like) structures.

Mitochondrial inheritance phenotypes were quantified as described previously (Hermann *et al.* 1997; Roeder *et al.* 1998) in *mdm20* suppressor strains transformed with the pDO12 plasmid (Otsuga *et al.* 1998), which expresses a mitochondrial matrix-targeted Cox4-green fluorescent protein (GFP) fusion protein. Overnight cultures grown at 25° in synthetic medium were diluted to an OD_{600} of ≤1.0 in fresh medium and grown an additional 2–3 hr at 25° or 37° before scoring. Digital microscopic images of cells were acquired as described previously (Otsuga *et al.* 1998).

The Lat-A halo assay was performed essentially as described by Ayscough *et al.* (1997) except that plates were seeded with a fixed number of cells (2.25×10^6) instead of a fixed volume of cell culture. Digital images of each plate were acquired and halo dimensions were determined using the application NIH Image V1.61 (http://rsb.info.nih.gov/nih-image). Two wild-type strains, JSY840 and JSY999 (Table 1), were used separately

or together in independent repetitions of the experiment as standards for Lat-A sensitivity. Mutant strains JSY3308, JSY3311, JSY3313, and JSY3315 (Table 1) were tested at least three times each. The five remaining *MDM20 DMT* strains were analyzed in less detail but demonstrated similar effects.

Computer analysis of suppressor mutations: Coordinate data and additional instructions for reconstructing structural models of actin monomers and polymers were obtained from the internet web site generously made available by M. Lorenz (http://ergo.mpimf-heidelberg.mpg.de/~michael/) or from the Protein Data Bank (PDB) (http://www.rcsb.org/pdb). Yeast actin monomers were visualized using the coordinate file '1YAG.pdb'. The file 'mdac.pdb', containing the structural coordinates for rabbit skeletal muscle actin (Lorenz *et al.* 1993), was used to build actin helices via the program 'helix.c'. This program constructed new coordinate files for actin polymers from monomer data. Coordinate files were converted into images by the application RasMac v2.6 [(c) 1994–1996, Roger Sayle; http://www.umass.edu/microbio/rasmol/]. Some additional modeling of mutant actin monomers was performed with the aid of the program 'O' (Jones *et al.* 1991) using coordinates '1ATN.pdb' and '1YAG.pdb'.

To find actin homologues with amino acid (aa) variations at positions equivalent to residues L221, Q314, G308 in yeast, we made use of the online application, PatScan (http://www-unix.mcs.anl.gov/compbio/PatScan/HTML/). Short Act1p sequences (11–14 aa) encompassing the residues of interest were submitted, along with the search parameters to return all matching sequences from the Swiss-Prot database containing between zero and three mismatches. At least 187 nonredundant homologous sequences, all from actin genes, were returned for each segment of Act1p submitted. Six of 189 homologues contained an amino acid difference at L221, 1 of 187 at G308, and 54 of 187 at Q314.

RESULTS

Isolation of *DMT1* and *DMT2*: In an effort to identify loci that interact genetically with yeast *MDM20*, we designed a selection for **d**ominant suppressor-of-***m****dm20* (*DMT*) mutations. The strategy of seeking only dominant mutations was adopted to increase the stringency of the selection. As previously reported (Hermann *et al.* 1997; Hermann 1998), overexpression of the Tpm1 protein partially suppressed the *mdm20* conditional growth defect in haploid cells. This suppression was greatly reduced in homozygous *mdm20/mdm20* diploid strains (Hermann 1998). To minimize the probability of isolating mutations that suppressed *mdm20* by simply increasing the steady-state level of Tpm1p, we screened for dominant suppressors in *mdm20/mdm20* diploids.

We isolated nine spontaneous mutations capable of suppressing the *mdm20/mdm20* temperature-sensitive growth defect—three mutations in JSY1371 (*mdm20*Δ/*mdm20*Δ; Table 1) and six mutations in JSY1372 (*mdm20-1/mdm20-1*; Table 1). Subsequent genetic analysis revealed no allele-specific suppression among the new *DMT* mutations; all nine were able to dominantly suppress the 37° growth defect in diploids homozygous for *mdm20*Δ (Figure 1). The level of growth restored by the suppressor mutations in diploids varied from weak to nearly wild type depending on the *DMT* allele present (Figure 1). In addition, all of the *DMT* mutations suppressed temperature-sensitive growth defects of the *mdm20*Δ allele in haploid strains (Figure 2).

Pairwise crosses of *DMT mdm20* strains and subsequent tetrad analysis revealed that the original *DMT* mutations segregated 2:2 and defined two linkage groups, *DMT1* and *DMT2* (Tables 2 and 3). As described below, the six alleles of *DMT1* and the three alleles of *DMT2* correspond to new alleles of the *ACT1* and *TPM1* genes, respectively.

***DMT1* mutations fall in the *ACT1* gene:** Two observations led us to suspect that *DMT1* mutations fall in *ACT1*. First, our attempts to clone the *DMT1-4* allele using a genomic library constructed from a *DMT1-4* strain were unsuccessful, despite the fact that auxotrophic markers such as *TRP1* and *ADE2* were readily cloned from the same library (data not shown). This observation led us to suspect that yeast cells might be adversely affected by extra copies of the gene underlying *DMT1* mutations, just as they are by an increased dosage of *ACT1* (cited in Huffaker *et al.* 1987; Liu *et al.* 1992; Magdolen *et al.* 1993). Second, both *DMT1* and *DMT2* suppressors stabilized actin cables in *mdm20* cells (see below). A recent study showed that this phenotype could result from certain mutations in the *ACT1* gene. Belmont and Drubin (1998) described a mutation in *ACT1*, V159N, which restored actin cable-like structures in *mdm20* mutants (though it did not rescue the *mdm20* conditional growth phenotype). To determine whether the *DMT1* mutations were genetically linked to *ACT1*, the *DMT1* strains were crossed to a strain containing a functional, *HIS3*-marked copy of the *ACT1* gene (JSY3079, *ACT1::HIS3*, Table 1). The segregation of histidine prototrophy and *mdm20* conditional growth suppression was then analyzed in tetrads. As summarized in Table 2, the *DMT1* mutations were tightly linked to the *ACT1* locus. In addition, sequence analysis revealed that all of the *DMT1* alleles contained mutations in the *ACT1* gene that altered the predicted amino acid sequence of actin (Table 2). On the basis of these findings, we assigned each of the *DMT1* mutations a new *ACT1* allele number (Table 2).

***DMT2* mutations fall in the *TPM1* gene:** The *TPM1* gene was previously identified as a multicopy suppressor of *mdm20* (Hermann *et al.* 1997). To rule out the possibility that the *DMT* suppressors were regulators of *TPM1* expression, we used Western blot analysis to compare the steady-state level of Tpm1p in wild-type, *mdm20*Δ, and *mdm20*Δ *DMT* strains. The steady-state level of Tpm1p in all of the strains was similar. However, migration of Tpm1p was faster than wild type in protein extracts prepared from *DMT2-1* and *DMT2-2* strains and slower in extracts prepared from the *DMT2-3* strain, suggesting that *DMT2* lesions might fall in the *TPM1* coding region (data not shown). Genetic linkage and sequence analysis of the *TPM1* locus from *DMT2* strains verified that *DMT2* mutations are new alleles of *TPM1*

TABLE 1

***S. cerevisiae* strains used in this study**

Strain	Genotype
JSY840	*MAT***a** *leu2Δ1 ura3-52*
JSY999[a]	*MATα his3Δ200 leu2Δ1 ura3-52*
JSY1065[a]	*MATα his3Δ200 leu2Δ1 ura3-52 mdm20Δ::LEU2*
JSY1081	*MATα his3Δ200 leu2Δ1 ura3-52 tpm1Δ::HIS3*
JSY1371	*MAT***a**/*MATα his3Δ200/his3Δ200 leu2Δ1/leu2Δ1 ura3-52/ura3-52 mdm20Δ::LEU2/mdm20Δ::LEU2*
JSY1372	*MAT***a**/*MATα his3Δ200/his3Δ200 leu2Δ1/leu2Δ1 ura3-52/ura3-52 mdm20-1/mdm20-1*
JSY1373	*MAT***a**/*MATα his3Δ200/his3Δ200 leu2Δ1/leu2Δ1 ura3-52/ura3-52*
JSY3079	*MAT***a** *his3Δ200 leu2Δ1 ura3-52 mdm20Δ:LEU2 ACT1::HIS3*
JSY3094	*MAT***a** *his3Δ200 leu2Δ1 ura3-52 mdm20Δ::LEU2*
JSY3227	*MAT***a**/*MATα his3Δ200/his3Δ200 leu2Δ1/leu2Δ1 ura3-52/ura3-52 mdm20Δ::LEU2/mdm20Δ::LEU2 DMT1-1/+*
JSY3228	*MAT***a**/*MATα his3Δ200/his3Δ200 leu2Δ1/leu2Δ1 ura3-52/ura3-52 mdm20Δ::LEU2/mdm20Δ::LEU2 DMT1-2/+*
JSY3229	*MAT***a**/*MATα his3Δ200/his3Δ200 leu2Δ1/leu2Δ1 ura3-52/ura3-52 trp1Δ63/+ mdm20Δ::LEU2/mdm20Δ::LEU2 DMT1-3/+*
JSY3230	*MAT***a**/*MATα his3Δ200/his3Δ200 leu2Δ1/leu2Δ1 ura3-52/ura3-52 lys2Δ202/+ mdm20Δ::LEU2/mdm20Δ::LEU2 DMT1-4/+*
JSY3231	*MAT***a**/*MATα his3Δ200/his3Δ200 leu2Δ1/leu2Δ1 ura3-52/ura3-52 trp1Δ63/+ mdm20Δ::LEU2/mdm20Δ::LEU2 DMT1-5/+*
JSY3232	*MAT***a**/*MATα his3Δ200/his3Δ200 leu2Δ1/leu2Δ1 ura3-52/ura3-52 lys2Δ202/+ mdm20Δ::LEU2/mdm20Δ::LEU2 DMT1-6/+*
JSY3233	*MAT***a**/*MATα his3Δ200/his3Δ200 leu2Δ1/leu2Δ1 ura3-52/ura3-52 mdm20Δ::LEU2/mdm20Δ::LEU2 DMT2-1/+*
JSY3234	*MAT***a**/*MATα his3Δ200/his3Δ200 leu2Δ1/leu2Δ1 ura3-52/ura3-52 lys2Δ202/+ trp1Δ63/+ mdm20Δ::LEU2/mdm20Δ::LEU2 DMT2-2/+*
JSY3235	*MAT***a**/*MATα his3Δ200/his3Δ200 leu2Δ1/leu2Δ1 ura3-52/ura3-52 lys2Δ202/+ mdm20Δ::LEU2/mdm20Δ::LEU2 DMT2-3/+*
JSY3236	*MATα his3Δ200 leu2Δ1 ura3-52 mdm20Δ::LEU2 DMT1-1*
JSY3237	*MATα his3Δ200 leu2Δ1 ura3-52 mdm20Δ::LEU2 DMT1-2*
JSY3238	*MAT***a** *his3Δ200 leu2Δ1 trp1Δ63 ura3-52 mdm20Δ::LEU2 DMT1-3*
JSY3239	*MAT***a** *his3Δ200 leu2Δ1 lys2Δ202 ura3-52 mdm20Δ::LEU2 DMT1-4*
JSY3240	*MAT***a** *his3Δ200 leu2Δ1 trp1Δ63 ura3-52 mdm20Δ::LEU2 DMT1-5*
JSY3241	*MATα his3Δ200 leu2Δ1 lys2Δ202 ura3-52 mdm20Δ::LEU2 DMT1-6*
JSY3242	*MATα his3Δ200 leu2Δ1 ura3-52 mdm20Δ::LEU2 DMT2-1*
JSY3243	*MAT***a** *his3Δ200 leu2Δ1 lys2Δ202 trp1Δ63 ura3-52 mdm20Δ::LEU2 DMT2-2*
JSY3244	*MAT***a** *his3Δ200 leu2Δ1 lys2Δ202 ura3-52 mdm20Δ::LEU2 DMT2-3*
JSY3289	*MATα his3Δ200 leu2Δ1 ura3-52 mdm20-1 DMT1-3*
JSY3290	*MATα his3Δ200 leu2Δ1 ura3-52 mdm20-1 DMT1-5*
JSY3307	*MAT***a** *his3Δ200 leu2Δ1 ura3-52 DMT1-1*
JSY3308	*MATα leu2Δ1 ura3-52 DMT1-2*
JSY3309	*MATα his3Δ200 leu2Δ1 ura3-52 DMT1-3*
JSY3310	*MATα his3Δ200 leu2Δ1 ura3-52 DMT1-4*
JSY3311	*MATα his3Δ200 leu2Δ1 ura3-52 DMT1-5*
JSY3312	*MATα leu2Δ1 ura3-52 DMT1-6*
JSY3313	*MATα his3Δ200 leu2Δ1 ura3-52 DMT2-1*
JSY3314	*MATα his3Δ200 leu2Δ1 ura3-52 DMT2-2*
JSY3315	*MAT***a** *leu2Δ1 ura3-52 DMT2-3*

All strains are congenic with FY10 (Winston *et al.* 1995).
[a] Hermann *et al.* (1997).

(Table 3). Accordingly, each *DMT2* mutation has been assigned a new *TPM1* allele designation (Table 3). The new *ACT1* and *TPM1* allele numbers will be used in all subsequent discussion of the *DMT* mutations (refer to Tables 2 and 3). In addition, because we observed significant phenotypic overlap among the six *ACT1* suppressor alleles and among the three *TPM1* alleles, data generated with two representative alleles from each group (*ACT1-202*, *ACT1-205* and *TPM1-3*, *TPM1-5*) are shown in the remainder of this study.

Dominant *ACT1* and *TPM1* alleles partially restore actin cables and rescue mitochondrial inheritance defects in *mdm20* cells: The *ACT1* and *TPM1* suppressor alleles restored short actin cables in *mdm20* cells. In wild-type cells stained with Alexa568-conjugated phalloidin at 25°, full-length actin cables extended from the tip of the bud, through the bud neck, and across the length of the mother cell to its distal tip (Figure 3, B and G). In *mdm20* cultures, however, only ~12% of the cells contained structures that resembled actin cables

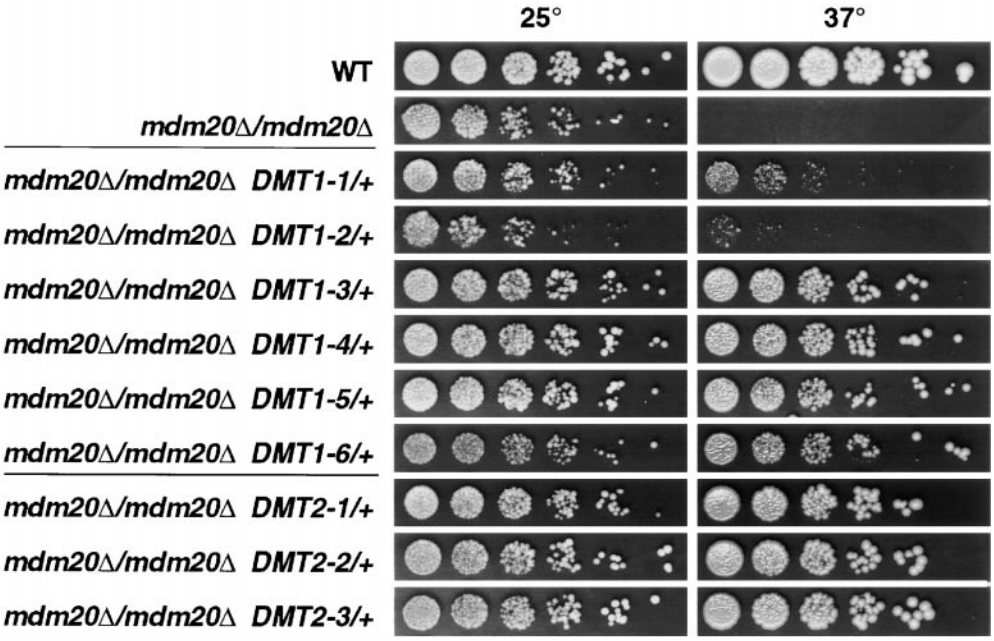

FIGURE 1.—*DMT1* and *DMT2* dominant mutations suppress the temperature-sensitive growth defect of homozygous *mdm20/mdm20* diploids. From top to bottom, the strains pictured are JSY1373, JSY1371, and JSY3227–3235 (Table 1). All but JSY1373 (WT) are homozygous for the deletion allele of *mdm20* (*mdm20*Δ). Among the suppressor-carrying strains, only JSY3227 (*DMT1-1*), JSY3228 (*DMT1-2*), and JSY3233 (*DMT2-1*) were isolated directly from the original selection. Alleles *DMT1-3* through *DMT1-6*, as well as *DMT2-2* and *DMT2-3*, were isolated in the *mdm20-1/mdm20-1* background and the corresponding *mdm20*Δ*/mdm20*Δ strains were constructed through subsequent crosses. All strains were serially diluted, spotted on YPD medium, and grown for 3 days at 25° or 37°.

(Figure 3, D and G). These cells typically had one or two extremely short, fluorescing rods very close to the bud neck that appeared to be rudimentary actin cables (not shown). The remaining 88% of budded *mdm20* cells contained no detectable actin cables, though actin patches were still present. In contrast, when *ACT1* or *TPM1* suppressor alleles were introduced into *mdm20* strains (*e.g.*, *mdm20*Δ *ACT1-202*, Figure 3F), the percentage of cells containing actin cable-like structures increased to 80% or more, depending on the allele (Figure 3G). In the majority of these cells, the suppressor mutations did not completely restore actin cables since cables still appeared shorter and less brightly stained than those in wild-type cells. As a result, images of these cables could be obtained only by overexposing actin patches in these cells (Figure 3F). The observation that restored actin cables were shorter and less bright than wild-type cables was verified in indirect immunofluorescence experiments (data not shown).

In similar experiments, we found that the new *ACT1* mutations do not restore actin cables in *tpm1*Δ mutant cells (data not shown). These results suggest that the *ACT1* alleles do not function by eliminating the need for Tpm1p *in vivo*.

The dominant *ACT1* and *TPM1* suppressor mutations also rescued the mitochondrial inheritance defects associated with *mdm20* cells. In wild-type cells grown at 25° or 37°, mitochondrial membranes visualized with the green fluorescent protein (Cox4-GFP) were transported into essentially 100% of the emerging buds (Figure 4, B and G). In contrast, only 72% of *mdm20* buds formed at 25° and 46% of *mdm20* buds formed at 37° inherited GFP-labeled mitochondrial compartments (Figure 4, D and G). When *mdm20* mutants also carried an *ACT1*

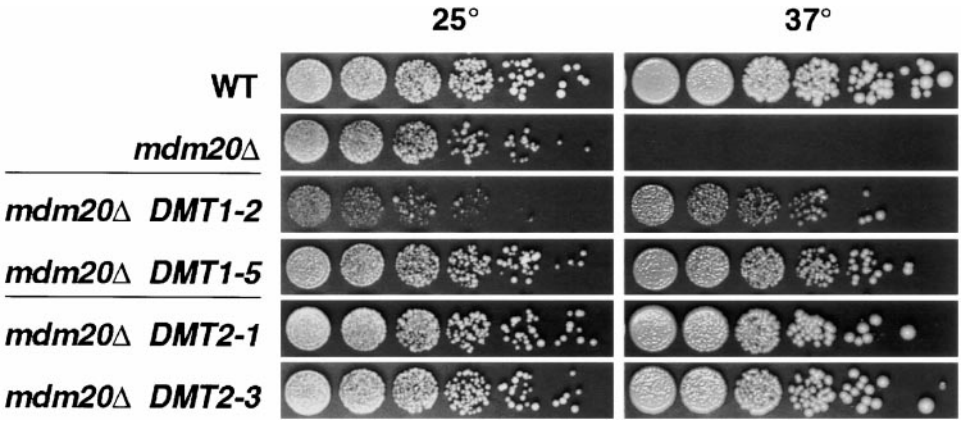

FIGURE 2.—*DMT1* and *DMT2* mutations suppress the temperature-sensitive growth defect of *mdm20*Δ haploids. From top to bottom the strains pictured are JSY999, JSY1065, JSY3237, JSY3240, JSY3242, and JSY3244 (Table 1). All strains were serially diluted, spotted on YPD medium, and grown for 3 days at 25° or 37°.

TABLE 2

Genetic and molecular evidence that *DMT1* is *ACT1*

DMT1 allele	Freq. of recombination[a] with *ACT1::HIS3* allele[b]	Sequence change at the *ACT1* locus	*ACT1* allele designation
DMT1-1	0/65	L221F	*ACT1-201*
DMT1-2	0/58	Q314R	*ACT1-202*
DMT1-3	0/56	G308C	*ACT1-203*
DMT1-4	ND	G308C	*ACT1-204*
DMT1-5	0/78	G308V	*ACT1-205*
DMT1-6	ND	G308V	*ACT1-206*

ND, not done.

[a] Recombination frequencies were obtained by counting individual spores whose genotypes could be unambiguously deduced.

[b] JSY3079, carrying the *HIS3*-marked *ACT1* allele, was crossed to *DMT1* mutant strains JSY3236, JSY3237, JSY3289, and JSY3290 (Table 1). The presence of a *DMT1* allele was indicated by suppression of the *mdm20* temperature-sensitive (ts) growth defect.

or *TPM1* suppressor mutation (*e.g.*, *mdm20*Δ *ACT1-202*, Figure 4F) the percentage of buds that inherited mitochondria increased to >95% at 25° and >90% at 37° (Figure 4G).

***ACT1* and *TPM1* suppressor alleles cause a small increase in Lat-A resistance:** To determine whether the new suppressor mutations conferred phenotypes on their own, haploid and homozygous diploid yeast strains carrying wild-type *MDM20* and either *ACT1* or *TPM1* suppressor mutations were subjected to a number of different assays. Previous studies indicated that yeast strains with actin cytoskeleton defects often display increased sensitivity to high osmolarity and/or extreme temperatures (Novick and Botstein 1985; Huffaker *et al.* 1987; Chowdhury *et al.* 1992; Winsor and Schiebel 1997). The *ACT1* and *TPM1* suppressor strains, however, grew as well as wild type on medium supplemented with 0.9 M NaCl and at temperatures ranging as high as 37° and as low as 13° (data not shown). Moreover, both cell morphology and mitochondrial inheritance in these strains were indistinguishable from wild type, and staining with Alexa568 phalloidin revealed no gross defects in actin organization (data not shown).

Despite the absence of visible actin organizational defects, cells carrying *ACT1* or *TPM1* suppressor alleles displayed a modest increase in actin cytoskeleton stability as measured by resistance to the actin-disrupting drug, Lat-A. Lat-A inhibits actin filament formation by sequestering actin monomers (Coué *et al.* 1987) and is lethal to yeast cells at high concentrations. When filter discs containing different concentrations of Lat-A are placed on a lawn of growing cells, a halo of growth inhibition (lethal concentration zone) becomes visible around each disc. The size of this halo provides a sensitive measure of a strain's resistance to the drug (Ayscough *et al.* 1997). *MDM20* strains carrying *ACT1* or *TPM1* suppressor alleles consistently produced slightly smaller halos than wild-type strains in response to equivalent concentrations of Lat-A (Figure 5, A, B, and E) indicating that the stability of actin structures was increased slightly in these strains.

An increased resistance to Lat-A was the only pheno-

TABLE 3

Genetic and molecular evidence that *DMT2* is *TPM1*

DMT2 allele	Freq. of recombination[a] with *tpm1*Δ*::HIS3* allele[b]	Sequence change at the *TPM1* locus	*TPM1* allele designation
DMT2-1	ND	S112F	*TPM1-3*
DMT2-2	0/20	S112Y	*TPM1-4*
DMT2-3	0/23	at**a** → at**g** (codon $^{-}$7)[c]	*TPM1-5*

ND, not done.

[a] Recombination frequencies were obtained by counting individual spores whose genotypes could be unambiguously deduced.

[b] JSY1081, carrying the selectable *HIS3* gene at the *TPM1* locus, was crossed to *DMT2* mutant strains JSY3243 and JSY3244 (Table 1). The presence of a *DMT2* allele was indicated by suppression of the *mdm20* ts growth defect.

[c] The *DMT2-3* mutation results in the addition of seven amino acids (MHTKKAT) to the Tpm1p N terminus. This has been verified by amino acid sequencing.

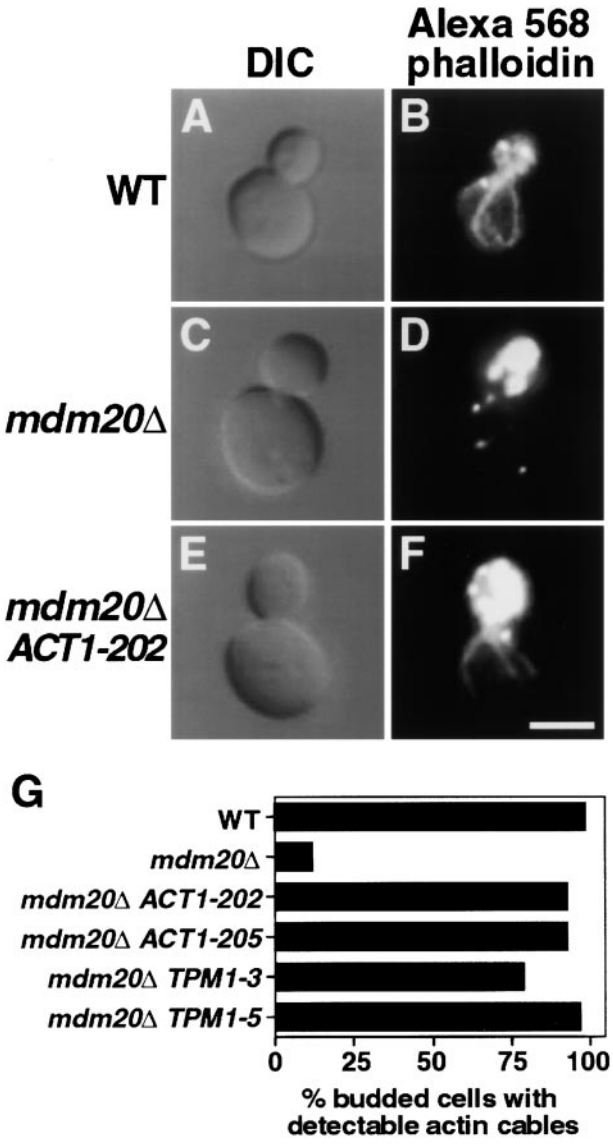

FIGURE 3.—Short actin cables emanate from the mother-bud neck in *mdm20*Δ mutants containing *ACT1* or *TPM1* suppressors. (A and B) Wild-type (JSY999), (C and D) *mdm20*Δ (JSY3094), and (E and F) *mdm20*Δ *ACT1-202* (JSY3237) cells were grown at 25°, stained with Alexa568 phalloidin and visualized by differential interference contrast (DIC) or fluorescence microscopy. Representative cells are shown. Bar, 2 μm. (G) Quantification of actin cable restoration. Wild-type (JSY999) and mutant cells carrying *mdm20*Δ alone (JSY3094) or in combination with a suppressor mutation (JSY3237, JSY3240, JSY3242, and JSY3244) were stained with Alexa568 phalloidin to visualize actin cables and patches. Budded cells were evaluated for the presence or absence of wild-type actin cables or cable-like structures. For each strain listed, the percentages represent the average of at least two separate experiments ($n \geq 225$).

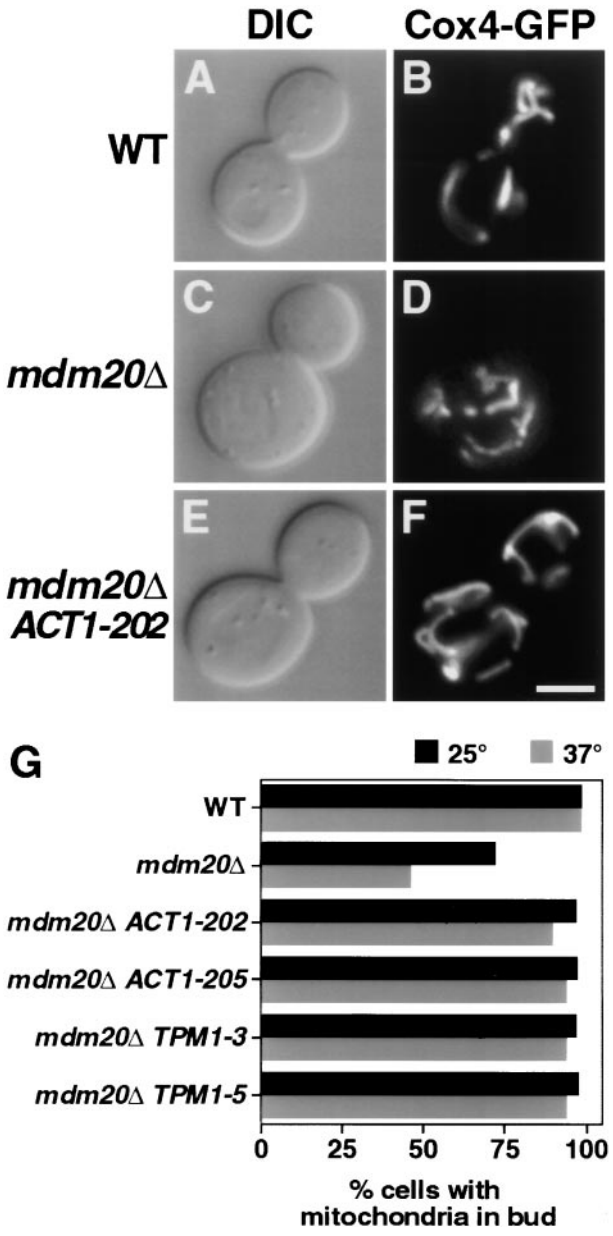

FIGURE 4.—Mitochondrial inheritance is restored in *mdm20*Δ cells containing *ACT1* or *TPM1* suppressors. GFP-labeled mitochondrial networks (pDO12; OTSUGA *et al.* 1998) were visualized in (A and B) wild-type (JSY999), (C and D) *mdm20*Δ (JSY3094), and (E and F) *mdm20*Δ *ACT1-202* (JSY3237) cells grown at 25° and shifted to 37° for 2–3 hr. DIC images (A, C, and E) and mitochondrial networks (B, D, and F) of representative cells are shown. Bar, 2 μm. (G) Quantification of mitochondrial inheritance defects. Wild-type (JSY999) and mutant cells carrying *mdm20*Δ alone (JSY3094) or *mdm20*Δ in combination with an *ACT1* or *TPM1* suppressor mutation (JSY3237, JSY3240, JSY3242, and JSY3244) were grown at 25° (solid bars) or 37° (shaded bars). Large-budded cells were scored for the presence or absence of mitochondria in buds. For each strain listed, the percentages represent the average of at least two separate experiments ($n \geq 125$).

type we detected in *MDM20* cells carrying the new *ACT1* and *TPM1* mutations. Like the other effects of these mutations, however, enhanced Lat-A resistance was more easily observed in an *mdm20* mutant background. Compared to wild type (Figure 5A), an *mdm20*Δ strain (Figure 5C) had very low Lat-A resistance and exhibited a large growth inhibition halo. Resistance was clearly increased when the *mdm20*Δ mutation was paired with

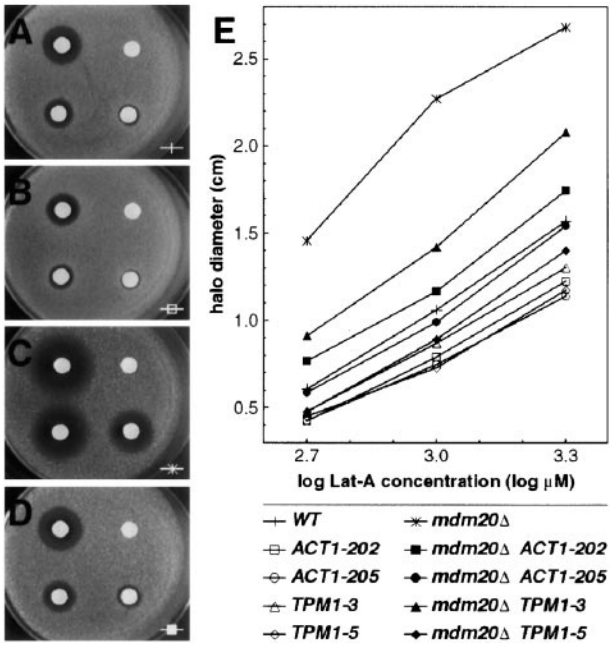

FIGURE 5.—Sensitivity to Lat-A is decreased by the new alleles of *ACT1* and *TPM1*. Filter discs infused with increasing concentrations of the actin-disrupting drug Lat-A (clockwise from top right: 0 mM, 0.5 mM, 1 mM, and 2 mM) were applied to fresh lawns of (A) wild-type (JSY999), (B) *MDM20 ACT1-202* (JSY3308), (C) *mdm20*Δ (JSY3094), and (D) *mdm20*Δ ACT1-202 (JSY3237) cells. The plates were grown at 25° for 4 days. The complete results of a typical Lat-A experiment are shown in E. Strains not pictured in A–D, but for which results are shown in E, are JSY3311, JSY3313, JSY3315, JSY3240, JSY3242, and JSY3244 (Table 1).

a suppressor allele of *ACT1* (Figure 5, D and E) or *TPM1* (Figure 5E).

DISCUSSION

In this study, we demonstrated that suppressors of *mdm20* reside in genes encoding two major structural components of the actin cytoskeleton, *ACT1* and *TPM1*. All nine mutations confer a dominant suppressor phenotype in diploid *mdm20* strains and are able to suppress mutant phenotypes of the *mdm20*Δ allele. Each of the suppressor mutations partially or fully rescues all of the *mdm20* phenotypes examined, including temperature-sensitive growth, loss of actin cables, defective mitochondrial inheritance, and Lat-A sensitivity. In an *MDM20* (wild-type) background, the mutations cause a small increase in Lat-A resistance. Although the suppressor mutations alter multiple amino acids in the Act1 and Tpm1 proteins, the behavior of each suppressor is similar with respect to the different phenotypes. Our analysis of the position and nature of the different mutations suggests that they all achieve their effect by modifying the same aspect of actin organization or function. Specifically, the *mdm20* suppressors appear to strengthen the interaction between actin and tropomyosin.

***mdm20* suppressor mutations in *ACT1*:** As shown in Table 2, the *mdm20* suppressor mutations in actin change the identities of residues L221, Q314, and G308. When these mutations are mapped onto a three-dimensional (3-D) model of the actin monomer (Figure 6, A–C, red), they form a small cluster at the junction of subdomains three and four (KABSCH *et al.* 1990; BOTSTEIN *et al.* 1997). The position of the mutations suggests that the substituted amino acids may affect the normal interactions of actin with the filament-binding protein tropomyosin.

LORENZ *et al.* (1995) used X-ray fiber diffraction data from oriented actin-tropomyosin gels to predict the residues of actin that are likely to be important for tropomyosin binding. When the predicted tropomyosin-binding residues are highlighted on the actin monomer (Figure 6, B and C, green) together with the *mdm20* suppressor mutations (red), the *mdm20* suppressor mutations fall within the predicted tropomyosin "footprint" and directly adjacent to several of the key tropomyosin-binding amino acids. The overlap between the tropomyosin-binding site and the *mdm20* suppressor mutations in actin is even more striking in a model of a short actin polymer (Figure 6D). When viewed in this manner, the tropomyosin contact points in each monomer align along the actin filament and the *mdm20* suppressor mutations clearly fall within the composite tropomyosin-binding site (note that a tropomyosin molecule spans multiple actin monomers).

At the structural level, the new mutations we have identified appear to cause only minor changes within the actin monomer. The L221F substitution increases the local bulkiness of the polypeptide chain by a small degree, as do the G308C and G308V substitutions. With respect to the changes at G308, however, the loss of flexibility normally provided by glycine at that position might actually be the more significant consequence of these mutations. Based on the crystal structure of actin, the Q314R mutation causes the loss of hydrogen bonds normally shared with T318 and V327, but the structural effects of this change should again be minor. Although the mutation at Q314 is the only one that adds a charged amino acid, all three of the substituted amino acids are located on the actin surface (polymer as well as monomer). This finding is consistent with the idea that the mutated residues exert their effect by altering the way actin interacts with one or more of its protein-binding partners.

Residues L221, G308, and Q314, like most in actin, are very highly conserved. In a survey of 187 actin homologues from a wide range of organisms (see MATERIALS AND METHODS), L221 had only six variants, all unique, and G308 had only one. Residue Q314 was changed in many homologues, but always to N, S, or T—never to R as we found in this study. In contrast, some of the variants at L221 were quite similar to the mutation we isolated at this position, L221F. Interestingly, two of the

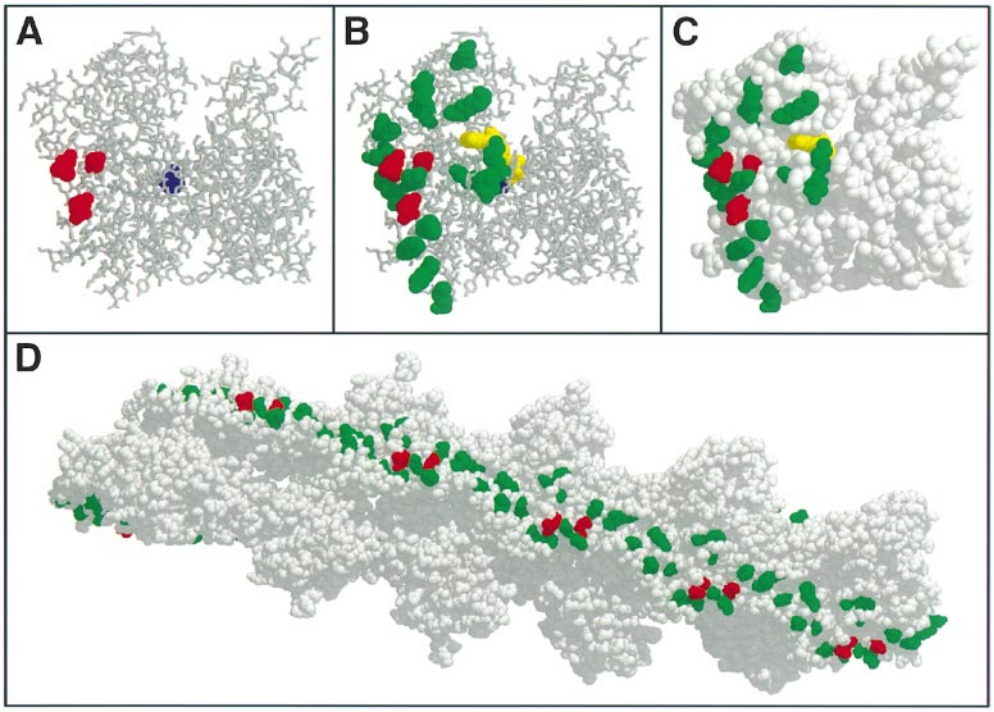

Figure 6.—The location of *mdm20* suppressor mutations on structural models of actin overlaps with the predicted binding site for tropomyosin. (A) Residues mutated in suppressor alleles of *ACT1* (L221, G308, and Q314) are highlighted in red on a 3-D model of yeast actin. The position of the previously reported V159N mutation is shown in blue (Belmont and Drubin 1998). In this view of the monomer, subdomains three and four correspond to the lower left and upper left quarters of the structure, respectively (Kabsch *et al.* 1990). On the identical structure in B, the polar residues of actin predicted to contribute to tropomyosin binding (Lorenz *et al.* 1995) are highlighted in green and a bound ATP molecule is shown in yellow. (C) A space-filling model of the structure shown in B. (D) A rabbit skeletal muscle actin 10-mer (Lorenz *et al.* 1993) showing the overlap of the *ACT1* suppressor mutations (red) with the predicted tropomyosin contact sites (green).

six L221 variants that were most similar came from the thermophilic fungus *Thermomyces lanuginosus* (F221; Wildeman 1988) and *Tetrahymena thermophila* (I221; Cupples and Pearlman 1986), organisms that thrive at temperatures up to 50° and 40°, respectively. Given that the L221F mutation allows budding yeast to overcome a temperature-sensitive growth defect, these observations raise the possibility that specific amino acid changes at residue L221 may be a recurring cellular strategy for increasing actin cytoskeleton stability at elevated temperatures.

One other actin mutation has been examined for its effect on *mdm20* mutant phenotypes. Belmont and Drubin (1998) showed that the V159N mutation in Act1p partially restores actin cables in *mdm20* cells, though it fails to rescue the *mdm20* temperature-sensitive growth defect. Cells containing the V159N mutation alone exhibit a variety of mutant actin phenotypes including slow growth at 25° and 37°, increased osmotic sensitivity, increased Lat-A resistance, and budding defects (Belmont and Drubin 1998). In contrast, the *ACT1* and *TPM1* suppressor mutations described in this report do not exhibit defects associated with disrupted actin function, with the exception of increased Lat-A resistance (Figure 5). Unlike the *mdm20* suppressors we isolated in subdomains three and four, the V159N mutation is located in the nucleotide binding cleft of the actin monomer (Figure 6, A and B) and has its primary effect on subdomain two (Belmont *et al.* 1999). Biochemical studies indicate that V159N retards actin filament depolymerization by preventing the actin conformational change that normally occurs after Pi release (Belmont *et al.* 1999). As a result, actin filament stability is increased in cells expressing V159N actin and these cells contain more robust actin cables and larger actin patches than normal. Although we have not yet performed biochemical studies, the phenotypes induced by our *mdm20* suppressor mutations and their positions on the actin monomer suggest that they do not increase filament stability by the same mechanism as V159N. One possible explanation for the different phenotypes induced by V159N compared to the *ACT1* and *TPM1* suppressor mutations is that the latter mutations potentially affect actin-tropomyosin interactions exclusively. Since tropomyosin is strictly localized to actin cables (Liu and Bretscher 1989), the actin-stabilizing effect of these mutations may be cable specific. In contrast, the V159N mutation affects actin dynamics in patches as well as cables (Belmont and Drubin 1998).

***mdm20* suppressor mutations in *TPM1*:** Tropomyosins are rod-shaped, dimeric coiled-coil proteins (Hitchcock-DeGregori 1994). They align end to end along the α-helical groove of actin filaments, each dimer spanning an integral number of actin monomers. Vertebrate

muscle tropomyosin spans seven monomers while nonmuscle isoforms span six (McLachlan and Stewart 1975; Côté 1983; Phillips *et al.* 1986). Yeast Tpm1p spans only five actin monomers (Liu and Bretscher 1989; Drees *et al.* 1995). Shorter isoforms are truncated at their N termini (Drees *et al.* 1995).

Since the 3-D form of a tropomyosin monomer is basically one continuous α-helix, there are few readily distinguishable structural domains (Greenfield and Hitchcock-DeGregori 1995). However, the comparison of different tropomyosin isoforms, particularly from vertebrates, has revealed that distinct regions of the protein are variable while others are more highly conserved. Most differences between vertebrate tropomyosin isoforms occur at the N or C termini or at a specific central region defined by a variable exon (exon VI; Lees-Miller and Helfman 1991; Lin *et al.* 1997). These three variable regions appear to be responsible for isoform-specific functions. The *mdm20* suppressor mutations we identified in *TPM1* encode changes at the N terminus and at residue S112 (Table 3). According to published alignments, S112 in yeast aligns with the central variable region of vertebrate tropomyosin isoforms (Drees *et al.* 1995; Lin *et al.* 1997). Thus, each of our *TPM1* suppressor mutations appears to fall within a region regularly exploited by evolution to modulate tropomyosin function.

The fact that we isolated two independent mutations at S112 suggests that this residue plays an important role in Tpm1p function. One obvious possibility is that S112 is phosphorylated. Several observations support the idea that S112 may be a target for phosphorylation. First, in the two closest Tpm1p homologues, *S. cerevisiae* Tpm2p and *Schizosaccharomyces pombe* Cdc8p, the positions analogous to S112 contain an S and an E residue, respectively (Balasubramanian *et al.* 1992; Drees *et al.* 1995). The negative charge on the glutamate side chain of *S. pombe* tropomyosin could be introduced in *S. cerevisiae* isoforms by the addition of a phosphate group to the corresponding serine residue. Second, several vertebrate tropomyosins are phosphorylated (Mak *et al.* 1978; Montarras *et al.* 1981; Heeley *et al.* 1982; Edwards and Romero-Herrera 1983), albeit at the C terminus rather than the central variable region (Mak *et al.* 1978). A vertebrate tropomyosin kinase has been identified but not well characterized (Montgomery and Mak 1984; deBelle and Mak 1987). Phosphorylation at the C termini of vertebrate tropomyosins is thought to be a mechanism by which troponin (in muscle cells; Heeley *et al.* 1989) and perhaps caldesmon (in nonmuscle cells) regulate tropomyosin-actin interactions. Although database searches of the *S. cerevisiae* genome reveal no clear homologues of troponin or caldesmon, it is possible that phosphorylation of S112 modulates the interaction of Tpm1p with actin via an analogous regulatory protein.

An alternative possibility is that phosphorylation of S112 normally influences the stability or conformation of the Tpm1p dimer. Coiled-coil proteins like tropomyosin are defined by the pseudoheptapeptide (heptad) repeat motif (Cohen and Parry 1986). Within each heptad, residues at the different positions, designated *a–g*, have typical characteristics. Positions *a* and *d* are normally filled by hydrophobic residues that form the core of the coiled-coil structure. In contrast, residues at positions *b*, *c*, *e*, *f*, and *g* are hydrophilic and solvent exposed in the dimerized protein. In the heptad repeat scheme of Tpm1p, S112 is located at an *a* position (Liu and Bretscher 1989), placing it at the interface of the Tpm1p dimer and suggesting that the primary effect of S112 phosphorylation could be to block standard coiled-coil interactions in this region of the protein. According to this scenario, the S112F and S112Y mutations we have isolated would eliminate Tpm1p phosphorylation and potentially increase dimer stability or induce a conformational change (Greenfield and Hitchcock-DeGregori 1995). Either result could improve binding of the Tpm1p dimer to actin filaments, ultimately increasing the stability of actin filaments and cables. We are currently examining the possibility that Tpm1p residue S112 is phosphorylated *in vivo*.

The *TPM1-5* mutation adds seven amino acids (MHTKKAT) to the N terminus of Tpm1p (Table 3). These additional amino acids might affect the end-to-end polymerization of Tpm1p dimers and/or the affinity of Tpm1p for the actin filament (Hitchcock-DeGregori 1994). The N-terminal extension might improve actin binding by mimicking N-terminal acetylation. Although it is not known whether yeast Tpm1p is acetylated at its N terminus, this modification is critical for strong actin binding in vertebrate muscle tropomyosin (Hitchcock-DeGregori and Heald 1987; Urbancikova and Hitchcock-DeGregori 1994). The same high level of actin binding can be induced in bacterially expressed, unacetylated tropomyosin by the addition of a few extra amino acids at the N terminus (Monteiro *et al.* 1994; Urbancikova and Hitchcock-DeGregori 1994). The composition of the fusion peptide appears to be unimportant and small peptides (≤11 aa) do not interfere with tropomyosin polymerization (Urbancikova and Hitchcock-DeGregori 1994). On the basis of these data, it seems possible that the addition of seven N-terminal amino acids might increase the actin-binding activity of Tpm1p and the stability of actin filaments.

Mechanism of *mdm20* suppression: The simplest explanation for our findings is that the *ACT1* and *TPM1* mutations we have isolated suppress *mdm20* defects by slightly adjusting normal actin-tropomyosin interactions such that actin filament and cable stability is enhanced. Since the *ACT1* and *TPM1* mutations are able to suppress mutant phenotypes in *mdm20* null strains, they can clearly bypass the requirement for *MDM20* function in yeast. However, our data leave open the possibility

that Mdm20p regulates interactions between the actin and tropomyosin proteins. In the future, biochemical assays can be used to study the actin assembly/turnover properties and actin filament-binding properties of the purified mutant actin and tropomyosin proteins described here. Additional biochemical studies using purified Mdm20p are necessary to determine whether this protein contributes primarily to actin-tropomyosin interactions or another aspect of actin filament dynamics.

We are grateful to Lisa Belmont, David Drubin, and Anthony Bretscher for strains, mutants, and plasmids and to Tatiana Karpova and John Cooper for goat anti-actin antibody. We especially thank Polycarpe Songfack for assistance with computer graphics and Jon Seger and Josh Cherry for sharing their statistical expertise. We also thank Anthony Bretscher, Michael Mathews, Denichiro Otsuga, Frank Whitby, and members of the Shaw laboratory for helpful discussions and careful review of the manuscript. This work was supported by grant GM-53466 from the National Institutes of Health (NIH) to J. Shaw. J. Singer was supported in part by a Huntsman Cancer Institute Graduate Fellowship and an NIH Predoctoral Genetics training grant (T32-GM07464). G. Hermann received support from an NIH Predoctoral Genetics training grant (T32-GM07464) and a University of Utah Graduate Research Fellowship.

Note added in proof: Since the initial submission of this manuscript, we have identified two additional *ACT1* alleles and one additional *TPM1* allele capable of suppressing *mdm20*. Preliminary analyses suggest that these mutations behave similarly to those described in this study. Indeed, two of the three are identical to previously identified mutations: *DMT1-7/ACT1-207* = G308C; *DMT2-4/TPM1-6* = S112Y. The remaining mutation is novel: *DMT1-8/ACT1-208* = L185F.

LITERATURE CITED

Adams, A. E. M., and D. Botstein, 1989 Dominant suppressors of yeast actin mutations that are reciprocally suppressed. Genetics **121:** 675–683.

Adams, A. E. M., and J. R. Pringle, 1991 Staining of actin with fluorochrome-conjugated phalloidin. Methods Enzymol. **194:** 729–731.

Ayscough, K. R., J. Stryker, N. Pokala, M. Sanders, P. Crews *et al.*, 1997 High rates of actin filament turnover in budding yeast and roles for actin in establishment and maintenance of cell polarity revealed using an actin inhibitor latrunculin-A. J. Cell Biol. **137:** 399–416.

Balasubramanian, M. K., D. M. Helfman and S. M. Hemmingsen, 1992 A new tropomyosin essential for cytokinesis in the fission yeast *S. pombe*. Nature **360:** 84–87.

Belmont, L. D., and D. G. Drubin, 1998 The yeast V159N actin mutant reveals roles for actin dynamics *in vivo*. J. Cell Biol. **142:** 1289–1299.

Belmont, L. D., A. Orlova, D. G. Drubin and E. H. Egelman, 1999 A change in actin conformation associated with filament instability after Pi release. Proc. Natl. Acad. Sci. USA **96:** 29–34.

Bender, A., and J. R. Pringle, 1991 Use of a screen for synthetic lethal and multicopy suppressee mutants to identify two new genes involved in morphogenesis in *Saccharomyces cerevisiae*. Mol. Cell. Biol. **11:** 1295–1305.

Boldogh, I., N. Vojtov, S. Karmons and L. A. Pon, 1998 Interaction between mitochondria and the actin cytoskeleton in budding yeast requires two integral mitochondrial outer membrane proteins, Mmm1p and Mdm10p. J. Cell Biol. **141:** 1371–1381.

Botstein, D., D. Amberg, J. Mulholland, T. Huffaker, A. Adams *et al.*, 1997 The yeast cytoskeleton, pp. 1–90 in *The Molecular Biology of the Yeast Saccharomyces*, edited by J. R. Pringle, J. R. Broach and E. W. Jones. Cold Spring Harbor Laboratory Press, Cold Spring Harbor, NY.

Catlett, N. L., and L. S. Weisman, 1998 The terminal tail region of a yeast myosin-V mediates its attachment to vacuole membranes and sites of polarized growth. Proc. Natl. Acad. Sci. USA **95:** 14799–14804.

Cheney, R. E., M. A. Riley and M. S. Mooseker, 1993 Phylogenetic analysis of the myosin superfamily. Cell Motil. Cytoskeleton **24:** 215–223.

Chowdhury, S., K. W. Smith and M. C. Gustin, 1992 Osmotic stress and the yeast cytoskeleton: phenotype-specific suppression of an actin mutation. J. Cell Biol. **118:** 561–571.

Cohen, C., and D. A. D. Parry, 1986 α-Helical coiled coils—a widespread motif in proteins. Trends Biochem. Sci. **11:** 245–248.

Côté, G. P., 1983 Structural and functional properties of the nonmuscle tropomyosins. Mol. Cell. Biochem. **57:** 127–146.

Coué, M., S. L. Brenner, I. Spector and E. D. Korn, 1987 Inhibition of actin polymerization by latrunculin A. FEBS Lett. **213:** 316–318.

Cupples, C. G., and R. E. Pearlman, 1986 Isolation and characterization of the actin gene from *Tetrahymena thermophila*. Proc. Natl. Acad. Sci. USA **83:** 5160–5164.

deBelle, I., and A. S. Mak, 1987 Isolation and characterization of tropomyosin kinase from chicken embryo. Biochim. Biophys. Acta **925:** 17–26.

Drees, B., C. Brown, B. G. Barrell and A. Bretscher, 1995 Tropomyosin is essential in yeast, yet the *TPM1* and *TPM2* products perform distinct functions. J. Cell Biol. **128:** 383–392.

Drubin, D. G., H. D. Jones and K. F. Wertman, 1993 Actin structure and function: roles in mitochondrial organization and morphogenesis in budding yeast and identification of the phalloidin-binding site. Mol. Biol. Cell **4:** 1277–1294.

Edwards, B. F., and A. E. Romero-Herrera, 1983 Tropomyosin from adult human skeletal muscle is partially phosphorylated. Comp. Biochem. Physiol. B **76:** 373–375.

Greenfield, N. J., and S. E. Hitchcock-DeGregori, 1995 The stability of tropomyosin, a two-stranded coiled-coil protein, is primarily a function of the hydrophobicity of residues at the helix-helix interface. Biochemistry **34:** 16797–16805.

Heeley, D. A., A. J. Moir and S. V. Perry, 1982 Phosphorylation of tropomyosin during development in mammalian striated muscle. FEBS Lett. **146:** 115–118.

Heeley, D. H., M. H. Watson, A. S. Mak, P. Dubord and L. B. Smillie, 1989 Effect of phosphorylation on the interaction and functional properties of rabbit striated muscle alpha-tropomyosin. J. Biol. Chem. **264:** 2424–2430.

Hermann, G. J., 1998 Mitochondrial inheritance and morphology in yeast. Ph.D. Thesis, University of Utah, Salt Lake City.

Hermann, G. J., and J. M. Shaw, 1998 Mitochondrial dynamics in yeast. Annu. Rev. Cell Dev. Biol. **14:** 265–303.

Hermann, G. J., E. J. King and J. M. Shaw, 1997 The yeast gene, *MDM20*, is necessary for mitochondrial inheritance and organization of the actin cytoskeleton. J. Cell Biol. **137:** 141–153.

Hill, K. L., N. L. Catlett and L. S. Weisman, 1996 Actin and myosin function in directed vacuole movement during cell division in *Saccharomyces cerevisiae*. J. Cell Biol. **135:** 1535–1549.

Hitchcock-DeGregori, S. E., 1994 Structural requirements of tropomyosin for binding to filamentous actin. Adv. Exp. Med. Biol. **358:** 85–96.

Hitchcock-DeGregori, S. E., and R. W. Heald, 1987 Altered actin and troponin binding of amino-terminal variants of chicken striated muscle alpha-tropomyosin expressed in *Escherichia coli*. J. Biol. Chem. **262:** 9730–9735.

Huffaker, T. C., M. A. Hoyt and D. Botstein, 1987 Genetic analysis of the yeast cytoskeleton. Annu. Rev. Genet. **21:** 259–284.

Johnston, G. C., J. A. Prendergast and R. A. Singer, 1991 The *Saccharomyces cerevisiae MYO2* gene encodes an essential myosin for vectorial transport of vesicles. J. Cell Biol. **113:** 539–551.

Jones, T. A., J. Y. Zou, S. W. Cowan and M. Kjeldgaard, 1991 Improved methods for binding protein models in electron density maps and the location of errors in these models. Acta Crystallogr. Sect. A **47:** 110–119.

Kabsch, W., H. G. Mannherz, D. Suck, E. F. Pai and K. C. Holmes, 1990 Atomic structure of the actin:DNase I complex. Nature **347:** 37–44.

Karpova, T. S., J. G. McNally, S. L. Moltz and J. A. Cooper, 1998 Assembly and function of the actin cytoskeleton of yeast: relationships between cables and patches. J. Cell Biol. **142:** 1501–1517.

Lazzarino, D. A., I. Boldogh, M. G. Smith, J. Rosand and L. A. Pon, 1994 Yeast mitochondria contain ATP-sensitive, reversible actin-binding activity. Mol. Biol. Cell **5:** 807–818.

Lees-Miller, J. P., and D. M. Helfman, 1991 The molecular basis for tropomyosin isoform diversity. Bioessays **13:** 429–437.

Lin, J. J., K. S. Warren, D. D. Wamboldt, T. Wang and J. L. Lin, 1997 Tropomyosin isoforms in nonmuscle cells. Int. Rev. Cytol. **170:** 1–38.

Liu, H., and A. Bretscher, 1989 Disruption of the single tropomyosin gene in yeast results in the disappearance of actin cables from the cytoskeleton. Cell **57:** 233–242.

Liu, H., and A. Bretscher, 1992 Characterization of *TPM1* disrupted yeast cells indicates an involvement of tropomyosin in directed vesicular transport. J. Cell Biol. **118:** 285–299.

Liu, H., J. Krizek and A. Bretscher, 1992 Construction of a *GAL1*-regulated yeast cDNA expression library and its application to the identification of genes whose overexpression causes lethality in yeast. Genetics **132:** 665–673.

Lorenz, M., D. Popp and K. C. Holmes, 1993 Refinement of the F-actin model against X-ray fiber diffraction data by the use of a directed mutation algorithm. J. Mol. Biol. **234:** 826–836.

Lorenz, M., K. J. Poole, D. Popp, G. Rosenbaum and K. C. Holmes, 1995 An atomic model of the unregulated thin filament obtained by X-ray fiber diffraction on oriented actin-tropomyosin gels. J. Mol. Biol. **246:** 108–119.

Magdolen, V., D. G. Drubin, G. Mages and W. Bandlow, 1993 High levels of profilin suppress the lethality caused by overproduction of actin in yeast cells. FEBS Lett. **316:** 41–47.

Mak, A., L. B. Smillie and M. Barany, 1978 Specific phosphorylation at serine-283 of alpha tropomyosin from frog skeletal and rabbit skeletal and cardiac muscle. Proc. Natl. Acad. Sci. USA **75:** 3588–3592.

McLachlan, A. D., and M. Stewart, 1975 Tropomyosin coiled-coil interactions: evidence for an unstaggered structure. J. Mol. Biol. **98:** 293–304.

Montarras, D., M. Y. Fiszman and F. Gros, 1981 Characterization of the tropomyosin present in various chick embryo muscle types and in muscle cells differentiated *in vitro*. J. Biol. Chem. **256:** 4081–4086.

Monteiro, P. B., R. C. Lataro, J. A. Ferro and F. C. Reinach, 1994 Functional alpha-tropomyosin produced in *Escherichia coli*. A dipeptide extension can substitute the amino-terminal acetyl group. J. Biol. Chem. **269:** 10461–10466.

Montgomery, K., and A. S. Mak, 1984 *In vitro* phosphorylation of tropomyosin by a kinase from chicken embryo. J. Biol. Chem. **259:** 5555–5560.

Novick, P., and D. Botstein, 1985 Phenotypic analysis of temperature-sensitive yeast actin mutants. Cell **40:** 405–416.

Otsuga, D., B. R. Keegan, E. Brisch, J. W. Thatcher, G. J. Hermann *et al.*, 1998 The dynamin-related GTPase, Dnm1p, controls mitochondrial morphology in yeast. J. Cell Biol. **143:** 333–349.

Peterson, J., Y. Zheng, L. Bender, A. Myers, R. Cerione *et al.*, 1994 Interactions between the bud emergence proteins Bem1p and Bem2p and Rho-type GTPases in yeast. J. Cell Biol. **127:** 1395–1406.

Phillips, G. N. J., J. P. Fillers and C. Cohen, 1986 Tropomyosin crystal structure and muscle regulation. J. Mol. Biol. **192:** 111–131.

Roeder, A. D., G. J. Hermann, B. R. Keegan, S. A. Thatcher and J. M. Shaw, 1998 Mitochondrial inheritance is delayed in *Saccharomyces cerevisiae* cells lacking the serine/threonine phosphatase, *PTC1*. Mol. Biol. Cell **9:** 917–930.

Sherman, F., G. R. Fink and J. B. Hicks, 1986 *Methods in Yeast Genetics*. Cold Spring Harbor Laboratory Press, Cold Spring Harbor, NY.

Simon, V. R., T. C. Swayne and L. A. Pon, 1995 Actin-dependent mitochondrial motility in mitotic yeast and cell-free systems: identification of a motor activity on the mitochondrial surface. J. Cell Biol. **130:** 345–354.

Simon, V. R., S. L. Karmon and L. A. Pon, 1997 Mitochondrial inheritance: cell cycle and actin cable dependence of polarized mitochondrial movements in *Saccharomyces cerevisiae*. Cell Motil. Cytoskeleton **37:** 199–210.

Urbancikova, M., and S. E. Hitchcock-DeGregori, 1994 Requirement of amino-terminal modification for striated muscle alpha-tropomyosin function. J. Biol. Chem. **269:** 24310–24315.

Wang, T., and A. Bretscher, 1995 The *rho*-GAP encoded by *BEM2* regulates cytoskeletal structure in budding yeast. Mol. Biol. Cell **6:** 1011–1024.

Wang, Y. X., N. L. Catlett and L. S. Weisman, 1998 Vac8p, a vacuolar protein with armadillo repeats, functions in both vacuole inheritance and protein targeting from the cytoplasm to vacuole. J. Cell Biol. **140:** 1063–1074.

Wildeman, A. G., 1988 A putative ancestral actin gene present in a thermophilic eukaryote: novel combination of intron positions. Nucleic Acids Res. **16:** 2553–2564.

Winsor, B., and E. Schiebel, 1997 An overview of the *Saccharomyces cerevisiae* microtubule and microfilament cytoskeleton. Yeast **13:** 399–434.

Winston, F., C. Dollard and S. L. Ricupero-Hovasse, 1995 Construction of a set of convenient *Saccharomyces cerevisiae* strains that are isogenic to S228C. Yeast **11:** 53–55.

Communicating editor: M. D. Rose